Journal of Alloys and Compounds 320 (2001) 40–45
www.elsevier.com/locate/jallcom

High pressure magnetic phase diagram of an antiferromagnetic Cr+0.50 at.% Re alloy single crystal

J.A.L. Lodya[1], H.L. Alberts*, P. Smit
Department of Physics, Rand Afrikaans University, PO Box 524, Auckland Park, Johannesburg 2006, South Africa

Received 18 January 2001; accepted 26 January 2001

Abstract

The pressure–temperature magnetic phase diagram of a Cr+0.50 at.% Re alloy single crystal has been obtained from high pressure ultrasonic wave velocity measurements. A triple point exists on the magnetic phase diagram where the incommensurate (I) and commensurate (C) spin-density-wave (SDW) phases coexist with the paramagnetic (P) phase. The ISDW–CSDW phase transition is a first-order transition while the CSDW–P and ISDW–P Néel transitions are continuous. Both the ISDW–CSDW/CSDW–ISDW and CSDW–P phase lines are nonlinear with exceptionally large pressure derivatives near the triple point pressure. Thermal expansion measurements on the crystal together with the high pressure measurements give a latent heat of 13.7 J mol^{-1} associated with the first-order ISDW–CSDW phase transition. The temperature dependence of the magnetovolume, $\Delta\omega$, has been observed to fit the equation $|\Delta\omega| = A_0 + A_1T^2 + A_2T^4$ fairly well in the CSDW phase.

Keywords: Magnetically ordered materials; Elasticity; Magnetic measurements; High pressure

JEL classification: 75.30.Kz; 75.50 Ee; 75.30.Fv

1. Introduction

The spin-density-wave (SDW) antiferromagnetism of Cr and its dilute alloys has attracted considerable interest during the past few decades due to the rich variety of magnetic phases observed in these systems [1]. In recent years the magnetic phase diagrams of dilute Cr alloys, both in the composition–temperature, (c–T), and pressure–temperature, (p–T), planes, have received particular attention [2–8]. The reason for this is partly the remarkable similarity observed experimentally between the (c–T) and (p–T) magnetic phase diagrams of these alloys. Renewed attention was also given recently to theoretical aspects of the magnetic phase diagrams of dilute Cr alloys [9,10].

When Cr is alloyed with group-7 transition metals Mn and Re the electron concentration is increased [1]. This brings the electron and hole octahedral Fermi surface sheets closer in dimensions thereby moving the SDW system from an incommensurate (I) SDW state to a commensurate (C) one. Depending on the Mn or Re content, Cr–Mn and Cr–Re alloy systems therefore display all known SDW phases; the longitudinal (L) ISDW, the transverse (T) ISDW and the CSDW phases. The (c–T) magnetic phase diagrams of the above two alloy systems were previously [1] determined completely. There appears a triple point on them where the ISDW, CSDW and paramagnetic (P) phases coexist. The ISDW–CSDW phase lines on the (c–T) magnetic phase diagrams of both the Cr–Mn and Cr–Re systems, interestingly, appear first-order like while the CSDW–P and ISDW–P transition lines are continuous.

Previous studies [11–13] of the (p–T) magnetic phase diagrams of Cr–Mn and Cr–Re alloys were done incompletely, giving information on only some of the phase lines. These incomplete studies were done on polycrystalline Cr–Mn and Cr–Re alloys. Polycrystalline material is not always the most suitable for such purposes. The reason is that in many polycrystalline Cr alloys the physical properties used to monitor the phase transitions either show only weak changes or, in some cases, no change at

*Corresponding author. Tel.: +27-11-489-2330; fax: +27-11-489-2339.
E-mail address: hla@na.rau.ac.za (H.L. Alberts).
[1]Permanent address: Vista University, Private Bag X09, Bertsham, Johannesburg 2013, South Africa.

0925-8388/01/$ – see front matter
PII: S0925-8388(01)00942-2

all in going through the phase transition temperatures. On the other hand, all physical properties studied so far in the few single crystalline dilute Cr alloys that are available show well defined anomalies in crossing all phase lines on their magnetic phase diagrams. Single crystalline materials are therefore better suited to obtain magnetic phase diagrams of dilute Cr alloys.

We succeeded in growing good quality Cr–Re alloy single crystals. As this alloy system is presently receiving attention in the literature [14–17] we report here the (p–T) magnetic phase diagram of a Cr+0.50 at.% Re alloy single crystal. This alloy has a concentration above the triple point concentration ($c \approx 0.3$ at.% Re), thereby exhibiting ISDW, CSDW or P phases at atmospheric pressure, depending on the temperature of the crystal.

2. Experimental

The Cr+0.50 at.% Re crystal is the same one previously [14] used for elastic constant measurements at atmospheric pressure. It is a crystal of good homogeneity and quality. Proof of this is found in the sharpness of the first-order ISDW–CSDW transition observed in thermal expansion measurements, not previously done on single crystalline Cr–Re alloys, of the present study. Thermal expansion measurements were taken at atmospheric pressure along the [100] direction using standard strain gauge techniques in the temperature range 77–450 K for both heating and cooling cycles. The rate of heating or cooling was about 0.06 K per min and the sensitivity for relative length changes was 3×10^{-7}. The thermal expansion of the Cr+0.50 at.% Re crystal was measured, as previously [1] done for other Cr alloys, relative to that of a Cr+5 at.% V alloy. The latter remains paramagnetic at all temperatures $T>0$ K and is usually used [1] to simulate the nonmagnetic state of antiferromagnetic (AF) dilute Cr alloys at all temperatures $T>0$ K. The measurements therefore directly give the magnetic contribution to the change in length.

Magnetic phase transition temperatures in the (p–T) magnetic phase diagram were obtained from anomalies observed in the hydrostatic pressure dependence of the longitudinal mode ultrasonic (10 MHz) wave velocity, propagating along the [110] direction in the crystal. Pressure measurements were done at different constant temperatures, kept constant to within 0.1 K. Some phase transition temperatures were also obtained from velocity–temperature measurements at different constant pressures, kept constant to within 10^{-3} GPa. Wave velocities were measured using standard ultrasonic pulse-echo-overlap techniques [18]. The resolution of the system for transit times was 1 part in 10^5 or better, making it ideally suited to monitor velocity changes due to applied pressure. Hydrostatic pressure in the range 0–0.24 GPa was generated using nitrogen gas as pressure medium.

3. Results

3.1. Thermal expansion

The thermal expansion measurements show that the magnetovolume, defined by

$$\Delta\omega = [V(\text{nonmagnetic}) - V(\text{magnetic})/V(\text{magnetic})]$$
$$= 3\Delta\ell/\ell(\text{measured}),$$

is negative for Cr+0.50 at.% Re. Figs. 1(a) and (b) show, respectively, the temperature dependencies of the absolute value of the magnetovolume, $|\Delta\omega|$, and of the thermal expansion coefficient, α, for the Cr+0.50 at.% Re crystal. The solid line in Fig. 1(b) represents the $\alpha - T$ curve for Cr+5 at.% V, giving the expected behaviour of Cr+0.50 at.% Re if it was nonmagnetic at all $T>0$ K.

The important feature in Fig. 1(a) is the sharp, nearly discontinuous, change in $|\Delta\omega|$ at the ISDW–CSDW phase transition. The transition is hysteretic, with a transition

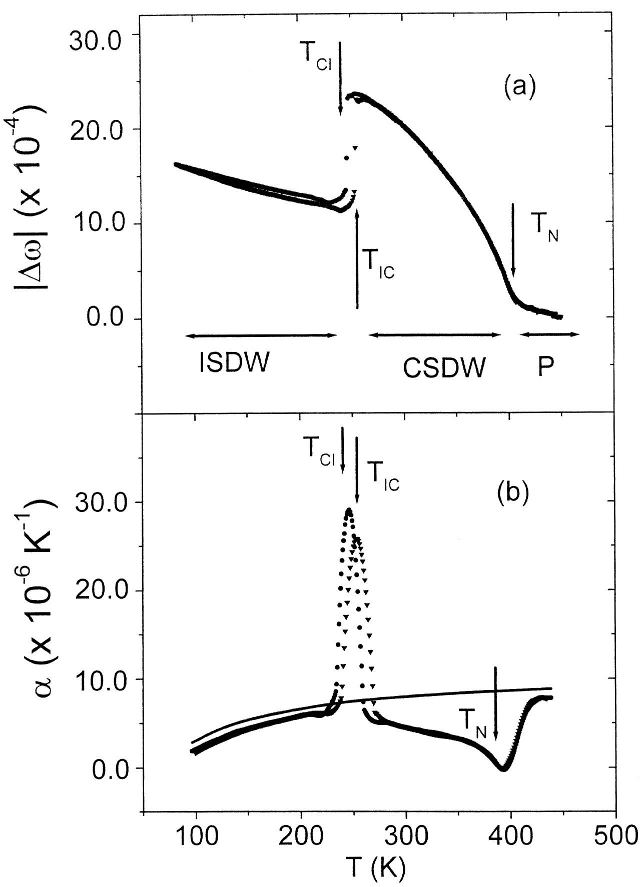

Fig. 1. Temperature dependence of (a) the absolute value of the magnetovolume, $|\Delta\omega|$, and (b) the coefficient of thermal expansion, α, for a Cr+0.50 at.% Re alloy single crystal. The triangles give the results for increasing temperature, and closed circles for decreasing temperature. The solid curve in (b) represents the data for Cr+5 at.% V giving the expected nonmagnetic behaviour of the Cr+0.50 at.% Re crystal.

width of about 7 K, characteristic of a first-order like transition. The sharpness of this transition indicates a crystal of good homogeneity. From Fig. 1(a) and (b) the ISDW–CSDW (on heating) transition temperature is $T_{IC}=(253\pm2)$ K and that of the CSDW–ISDW (on cooling) transition is $T_{CI}=(246\pm2)$ K.

3.2. Magnetic (p–T) phase diagram

Fig. 2(a) and 2(b) show typical results at constant temperatures of 267 K and 382 K, respectively, for the pressure dependence of the relative change in natural velocity, $\Delta W/W_0=(W_p-W_0)/W_0$, for longitudinal ultrasonic wave propagation along the [110] direction in the Cr+0.50 at.% Re crystal. Here W_p is the natural wave velocity defined [19] as the path length at zero applied pressure divided by the transit time at pressure p and W_0 that at atmospheric pressure. The temperature of 267 K was chosen to be close to the ISDW–CSDW/CSDW–ISDW phase transition temperatures and that of 382 K close to the CSDW–P Néel transition at atmospheric pressure.

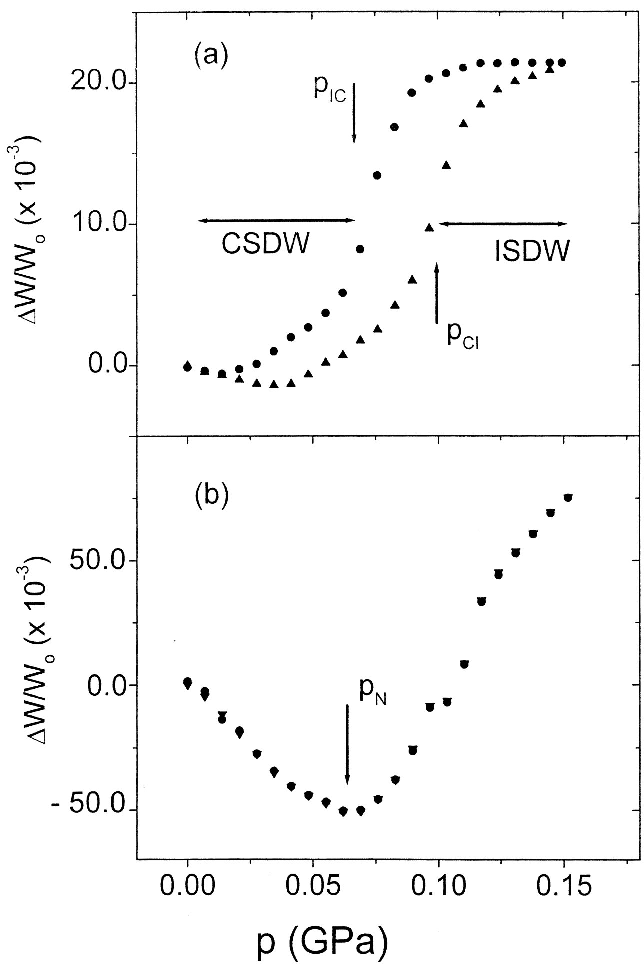

Fig. 2. Pressure dependence of the relative change in natural velocity, $\Delta W/W_0$, for a Cr+0.50 at.% Re alloy single crystal at constant temperatures of (a) 267 K and (b) 382 K. Triangles give the results for increasing pressure and closed circles for decreasing pressure.

On increasing the pressure p in Fig. 2(a), $\Delta W/W_0$ at first decreases slightly followed by a relatively sharp rise after which there is a tendency for $\Delta W/W_0$ to saturate. The cooling curve in Fig. 2(a) follows the same trend except for the presence of a large hysteresis effect. The relatively sharp changes in $\Delta W/W_0-p$ in Fig. 2(a) with increasing or decreasing pressure together with the accompanied hysteresis effect were taken as indicative of a first-order like CSDW–ISDW (on increasing p) or ISDW–CSDW (on decreasing p) transition induced by the applied pressure. The critical pressures p_{CI} and p_{IC} for the CSDW–ISDW and ISDW–CSDW transitions, respectively, were taken at the inflection points of the sharp rise (on increasing p) or the sharp descent (on decreasing p) on the $\Delta W/W_0-p$ curves of Fig. 2(a). Similar effects were previously [7,8] observed in Cr–Ru and Cr–Ir alloys. Fig. 2(a) gives $p_{CI}=(0.100\pm0.005)$ GPa and $p_{IC}=(0.070\pm0.005)$ GPa at 267 K. The hysteresis width in Fig. 2(a) is about 0.03 GPa.

At $T=382$ K (Fig. 2(b)) the $\Delta W/W_0-p$ curve initially shows a very large decrease in $\Delta W/W_0$ followed by a relatively broad minimum and a further sharp rise as p increases. No hysteresis effect on pressure cycling is observed in Fig. 2(b), showing a continuous second-order like pressure induced Néel transition from the CSDW to the P phase at pressure $p_N=(0.060\pm0.005)$ GPa. The transition pressure p_N was taken at the pressure of the minimum point in Fig. 2(b).

The hydrostatic pressure dependence of $\Delta W/W_0$ at different constant temperatures in the temperature range 250 K$<T<$300 K all reveal curves similar to those shown in the typical example of Fig. 2(a). These curves give points on the CSDW–ISDW and ISDW–CSDW phase lines of the (p–T) magnetic phase diagram shown in Fig. 3. For measurements at different constant temperatures in the range 350 K$<T<$400 K the $\Delta W/W_0-p$ curves are all

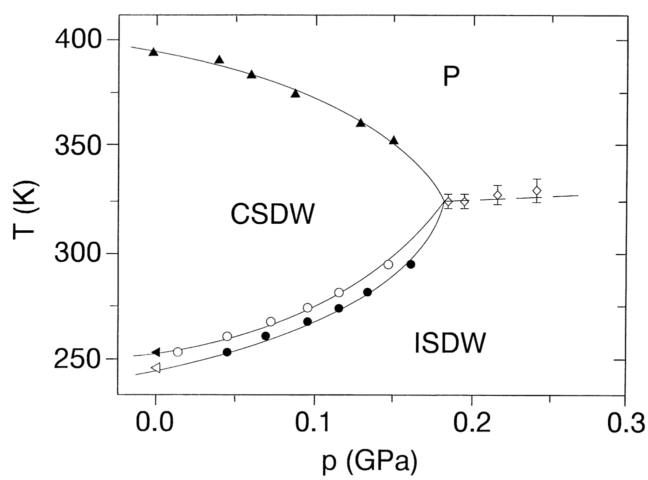

Fig. 3. Pressure–temperature magnetic phase diagram of a Cr+0.50 at.% Re alloy single crystal.

similar to that of Fig. 2(b), giving points on the CSDW–P phase line of Fig. 3.

The position of the ISDW–P phase line on the (p–T) magnetic phase diagram could not be obtained from $\Delta W/W_0 - p$ measurements at different constant temperatures. This is due to the gradient of this phase line being very close to zero. Measurements of the ultrasonic wave velocity as a function of temperature at different constant pressures above the triple point pressure in Fig. 3 were very suitable for this purpose. A typical example at a constant pressure of 0.22 GPa is shown in Fig. 4 where the Néel ISDW–P phase transition temperature is taken at the minimum point in the curve. The experimental points obtained in this way for the ISDW–P phase line are shown in Fig. 3.

The (p–T) magnetic phase diagram of Fig. 3 has a triple point at $T_t \approx 322$ K and $p_t \approx 0.19$ GPa where the ISDW, CSDW and P phases coexist. For $p < p_t$, either an ISDW or a CSDW phase is observed for $T < T_N$, depending on temperature, while only the ISDW phase is present at $p > p_t$ and $T < T_N$. The CSDW–ISDW and ISDW–CSDW phase transition lines in the (p–T) phase diagram are strikingly nonlinear, similarly as was found for a Cr+0.20 at.% Ir alloy [8] but in marked contrast with observations [7] in a Cr+0.3 at.% Ru single crystal. For the latter crystal all phase lines in the (p–T) magnetic phase diagram are linear lines. The pressure derivatives of T_{IC} and T_{CI} for the Cr+0.50 at.% Re crystal are large in the vicinity of the triple point in Fig. 3, giving $dT_{IC}/dp \approx 770$ K/GPa and $dT_{CI}/dp \approx 1200$ K/GPa compared to $dT_{IC}/dp = 277$ K/GPa and $dT_{CI}/dp = 333$ K/GPa for Cr+0.3 at.% Ru [7]. For the CSDW–P phase line the pressure derivative of T_N is negative, giving $dT_{CP}/dp \approx -810$ K/GPa close to the triple point compared to $dT_{CP}/dp = -358$ K/GPa for Cr+0.3 at.% Ru [7]. The initial values of $(dT_{CP}/dp)_{p=0} = -145$ K/GPa, $(dT_{IC}/dp)_{p=0} = +141$ K/GPa and $(dT_{CI}/dp)_{p=0} = +178$ K/GPa for Cr+0.50 at.% Re (Fig. 3) differ noticeably from corresponding values of -421 K/GPa, $+243$ K/GPa and $+406$ K/GPa, respectively, observed [8] for Cr+0.20 at.% Ir. The ISDW–P phase line in Fig. 3 is very flat, giving within experimental error a negligible pressure derivative.

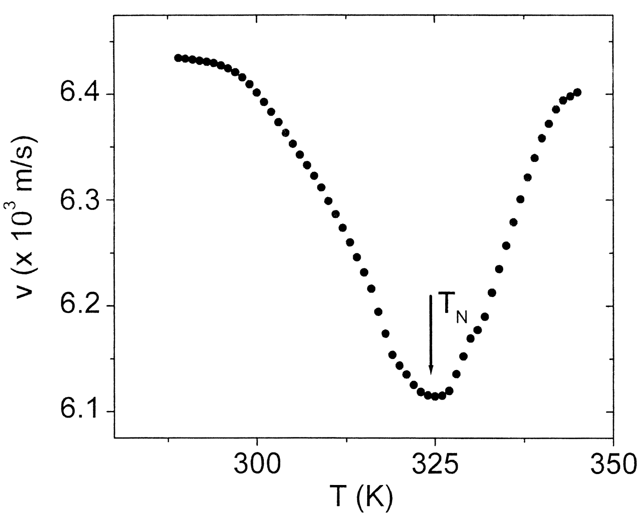

Fig. 4. Temperature dependence of the ultrasonic wave velocity, v, at a constant pressure of 0.22 GPa for a Cr+0.50 at.% Re alloy single crystal.

It is concluded that the magnetic phase diagrams in the pressure–temperature plane of dilute Cr alloys with the group-7 transition metal Re and with group-8 nonmagnetic transition metals Ru and Ir are similar in that they all exhibit a triple point where the CSDW, ISDW and P phases coexist. However, they differ in the linearity or nonlinearity of the phase lines and in the magnitude of the pressure derivatives of these lines. The magnitudes of the pressure derivatives as $p \to 0$ for the Cr+0.50 at.% Re crystal are markedly smaller than that for Cr–Ru and Cr–Ir, whereas they are noticeably larger in the former crystal than in the latter two near the triple point.

4. Discussion

The Clausius–Clapeyron equation was used to estimate the latent heat associated with the first-order ISDW–CSDW/CSDW–ISDW phase transition in the Cr+0.50 at.% Re crystal. From the thermal expansion measurements (Fig. 1) the volume change at this transition is observed to be $(V_{CSDW} - V_{ISDW})/V = (12 \pm 1) \times 10^{-4}$. Using this volume change and the average value $(dT_{IC}/dp)_{p=0} = +160$ K/GPa, the latent heat of the transition has been estimated as $L = 13.7$ J mol^{-1}, which is appreciably larger than the values $L = 5.8$ J mol^{-1} and $L = 4.5$ J mol^{-1} obtained [20] for the first-order I–C transition of two other Cr alloys with group-7 transition metals, namely Cr+0.45 at.% Mn and Cr+0.70 at.% Mn, respectively.

The thermal expansion measurements (Fig. 1) show that Cr+0.50 at.% Re expands when it is heated through the ISDW–CSDSW transition, giving $V_{CSDW} > V_{ISDW}$. A volume expansion stabilises the CSDW phase at the expense of the ISDW phase and results in a decrease of T_{IC} giving $dT_{IC}/dV < 0$ corresponding to $dT_{IC}/dp > 0$ [20], as observed in Fig. 3. As the CSDW phase has a larger unit cell volume than the ISDW phase it is expected [20,21] that the CSDW phase should be more sensitive to volume changes than the ISDW phase. This is consistent with the observation $|dT_{CP}/dp| > |dT_{IP}/dp|$ in Fig. 3.

According to a thermodynamic model [1] the magnetovolume of dilute Cr alloys should follow the equation

$$\Delta\omega = a_0 + a_1 t^2 + a_2 t^4, \qquad (1)$$

where $t = T/T_N$ is the reduced temperature. This equation was fitted successfully to the data of Fig. 1(a) in the temperature range $T_{IC} < T < T_N$ where the sample remains in the CSDW phase. The fit is shown in Fig. 5 and is rather good. The results give

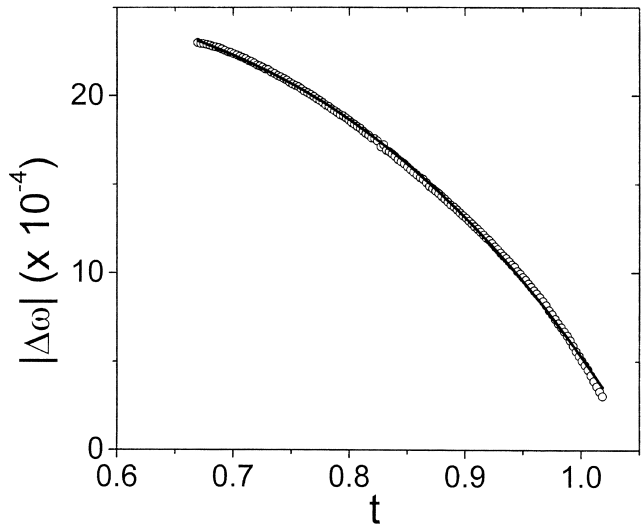

Fig. 5. The absolute value of the magnetovolume, $|\Delta\omega|$, as a function of reduced temperature, $t = T/T_N$, in the CSDW phase of a Cr+0.50 at.% Re alloy single crystal. The solid line is the best fit of the equation $|\Delta\omega| = a_0 + a_1 t^2 + a_2 t^4$.

$$a_0 = -(27.1\pm0.1)\times 10^{-4}$$
$$a_1 = -(1.4\pm0.4)\times 10^{-4}$$
$$a_2 = (22.8\pm0.3)\times 10^{-4}$$

From these values $(a_1 + a_2)/a_0 = -0.79$ which is reasonably close to the theoretical value of -1 [22].

It is usual to define [1] a magnetic Grüneisen parameter Γ_{IC} at the ISDW–CSDW phase transition, given by $\Gamma_{IC} = \mathrm{d}\ln T_{IC}/\mathrm{d}\omega$. From the present measurements of $\mathrm{d}T_{IC}/\mathrm{d}p$ on Cr+0.50 at.% Re a value $\Gamma_{IC} = +109$ is obtained, which is much smaller than the value $\Gamma_{IC} = +215$ observed [1] in a Cr+0.3 at.% Ru crystal. Γ_{IC} is also related to the magnetoelastic properties through [1]

$$\Gamma_{IC} = -\left[\frac{1}{\bar{B}T}\frac{\Delta B}{\Delta\beta}\right]_{IC}, \quad (2)$$

where ΔB and $\Delta\beta$ are, respectively, the discontinuities in the bulk modulus, B, and volume thermal expansion coefficient, β, at the ISDW–CSDW transition temperature and $\bar{B}$ is the mean bulk modulus at T_{IC}. Eq. (2) is strictly speaking valid for a continuous transition but was previously [1] applied to the first-order ISDW–CSDW transition of dilute Cr–Ru alloys. From the present measurements $\Delta\beta = \beta_{ISDW} - \beta_{CSDW} = -64\times10^{-6}$ for Cr+0.50 at.% Re and from previous [14] measurements on the same crystal $\Delta B = B_{ISDW} - B_{CSDW} = 0.2\times10^{11}$ Nm^{-2} and $\bar{B} = 1.7\times10^{11}$ Nm^{-2}. These values in Eq. (2) give $\Gamma_{IC} = +7$, which does not compare well at all with $\Gamma_{IC} = +109$ obtained above from the direct pressure measurements. The same situation was observed [1] for a Cr+0.3 at.% Ru crystal for which the respective values of Γ_{IC} are 5 and 215. The present measurements again demonstrate the serious limitations in using Eq. (2) to obtain magnetic Grüneisen parameters from magnetoelastic data near first-order like ISDW–CSDW phase transitions of dilute Cr alloys. At most Eq. (2) is useful in obtaining the correct sign of Γ_{IC}.

It was recently [23] shown theoretically that the strong pressure dependence of the properties of Cr is caused by two mechanisms. One is the nesting effect between the electron and hole Fermi surface sheets and the other is a new special mechanism arising from total energy calculations for body-centered cubic Cr. These calculations show that although the lowest energy state is nonmagnetic, a small expansion of the lattice induces an antiferromagnetic state. The strong pressure dependence of the properties is physically explained by combining the above two properties. Unfortunately, at this stage the theory does not provide useful equations to apply to the present measurements of the pressure derivatives of the magnetic phase transition temperatures.

Acknowledgements

Financial assistance from the South African National Research Foundation is acknowledged.

References

[1] E. Fawcett, H.L. Alberts, V.Yu. Galkin, D.R. Noakes, J.V. Yakhmi, Rev. Mod. Phys. 66 (1994) 25.
[2] E. Fawcett, Magnetism in metals, in: D.F. Morrow, J. Jensen, H.M. Ronnow (Eds.), The Royal Danish Academy of Science and Letters, Copenhagen, 1997.
[3] E. Fawcett, Why are the effects of pressure and composition change often similar in antiferromagnetic chromium alloys?, in: J.S. Faulkner, R.G. Jordan (Eds.), Metallic Alloys: Experimental and Theoretical Perspectives, Kluwer Academic Publishers, Dordrecht, 1994.
[4] J.A. Lodya, P. Smit, H.L. Alberts, J. Appl. Phys. 87 (2000) 4888.
[5] V.Yu. Galkin, P.C. de Camargo, N. Ali, E. Fawcett, J. Appl. Phys. 81 (1997) 4207.
[6] J.A. Fernandez-Baca, E. Fawcett, H.L. Alberts, V.Yu. Galkin, Y. Endoh, J. Appl. Phys. 81 (1997) 3877.
[7] H.A.A. Sidek, M. Cankurtaran, G.A. Saunders, P.J. Ford, H.L. Alberts, Phys. Lett. A172 (1993) 387.
[8] J. Martynova, H.L. Alberts, P. Smit, J. Magn. Magn. Mat. 187 (1998) 345.
[9] R.S. Fishman, X.W. Jiang, J. Appl. Phys. 81 (1997) 4201.
[10] R.S. Fishman, X.W. Jiang, S.H. Liu, Phys. Rev. B58 (1998) 414.
[11] A. Jayaraman, T.M. Rice, E. Bucher, J. Appl. Phys. 41 (1970) 869.
[12] J. Mizuki, Y. Endoh, Y. Ishikawa, J. Phys. Soc. Jpn. 51 (1982) 3497.
[13] A.K. Butylanko, N.S. Kobzenko, Ukr. Fiz. Zh. (Russian Ed.) 26 (1981) 199.
[14] A.H. Boshoff, H.L. Alberts, P. de V. du Plessis, A.M. Venter, J. Phys.: Condensed Matter 5 (1993) 5353.
[15] D.R. Noakes, E. Fawcett, B.J. Sternlieb, G. Shirane, J. Jankowska-Kisielinska, Physica B 241–243 (1998) 625.
[16] O.A. Bannykh, I.D. Marchukova, K.B. Povarova, Russ. Metall. (USA) 3 (1997) 43.
[17] L.M. Baklanova, L.M. Sheludchenko, V.Z. Enol'skii, Phys. Met. Metallogr. 85 (1998) 169.
[18] E.P. Papadakis, in: W.P. Mason, R.N. Thurston (Eds.), Physical Acoustics, Vol. 12, Academic Press, New York, 1976.

[19] R.N. Thurston, Proc. IEEE 53 (1965) 1320.
[20] B.M. Geerken, R. Griessen, G. Benediktsson, H.U. Åström, C. van Dijk, J. Phys. F: Met. Phys. 12 (1982) 1603.
[21] M. Cankurtaran, G.A. Saunders, Q. Wang, P.J. Ford, H.L. Alberts, Phys. Rev. B46 (1992) 14370.
[22] H.L. Alberts, J.A.J. Lourens, J. Phys.: Condens. Matter 4 (1992) 3835.
[23] P.M. Marcus, S-L. Qiu, V.L. Moruzzi, J. Phys.: Condens. Matter 10 (1998) 6541.